


**STANDARD ARTICLE**

# Characterization of Doppler spectrum of hepatic veins and correlation with structural and functional variables of the right ventricle in healthy dogs

Vinícius Bentivóglgio Costa Silva  | Tilde Rodrigues Froes | Elaine Mayumi Ueno Gil |  
 Marcela Wolf | Stephany Buba Lucina | Marlos Gonçalves Sousa

Department of Veterinary Medicine, Federal University of Paraná, Curitiba, Brazil

**Correspondence**

Vinícius Bentivóglgio Costa Silva, Department of Veterinary Medicine, Federal University of Paraná, Rua dos Funcionários 1540, 80035-050 Curitiba, Brazil.  
 Email: viniciusbcsilva@gmail.com

**Abstract**

**Background:** Spectral Doppler assessment of hepatic veins may provide information on heart function.

**Hypothesis/Objectives:** To assess the normal pattern of hepatic venous flow using spectral Doppler ultrasound examination; to correlate this information with structural and functional variables of the right ventricle (RV), and to analyze the impact of age, sex, body weight quartiles, heart rate, cardiac rhythm, and systolic arterial pressure on the results in healthy dogs.

**Animals:** Sixty-five healthy dogs.

**Methods:** Cross-sectional observational study. The direction and maximum velocity of each of the 4 possible components of venous flow were determined from pulsed-wave Doppler examination of the hepatic veins. In addition, structural and functional parameters (TAPSE, longitudinal strain, FAC%,  $S'$ ,  $E'_t/A'_t$  and  $E'_t/A'_t$ ) of the RV were evaluated.

**Results:** The same phase patterns for different waves were seen in all animals: A and V were retrograde waves, and S and D were anterograde waves. The velocity of the spectral waves increased with body weight ( $P < .05$ ) and could be correlated with functional indices of the RV. A significant difference was found when comparing morphometric indices with body weight quartiles ( $P < .05$ ). In addition, intra- and inter-observer assessments showed low variability. The mean duration of the examinations was 5.2 minutes.

**Conclusions and Clinical Importance:** Hepatic spectral Doppler findings can be correlated with systolic and diastolic indices of the RV and vary with body weight.

**KEYWORDS**

diagnosis, echocardiography, hemodynamics, ultrasonography

**Abbreviations:**  $A'$ , velocity of the tricuspid annulus systolic excursion in late diastole; BW, body weight; CV, coefficient of variation;  $E'$ , velocity of the tricuspid annulus systolic excursion in early diastole; FAC%, fractional area change; HR, heart rate; RV, right ventricle; S/D, ratio between the S and the D wave derived from hepatic venous Doppler;  $S'$ , velocity of the tricuspid annulus systolic excursion; SAP, systolic arterial pressure; TAPSE, tricuspid annular plane systolic excursion; TDI, tissue Doppler imaging.

**1 | INTRODUCTION**

Normal hepatic venous blood flow has low velocity and a pulsatile pattern that reflects the changes in right atrial pressure throughout the

This is an open access article under the terms of the Creative Commons Attribution-NonCommercial License, which permits use, distribution and reproduction in any medium, provided the original work is properly cited and is not used for commercial purposes.

© 2019 The Authors. *Journal of Veterinary Internal Medicine* published by Wiley Periodicals, Inc. on behalf of the American College of Veterinary Internal Medicine.

cardiac cycle. Therefore, assessment of hepatic veins using spectral Doppler could provide information about heart function.<sup>1</sup>

Although retrograde movement is seen, the majority of the hepatic venous blood flow must be antegrade and return to the heart chambers. The hepatic venous waves typically exhibit a 3-phase normal pattern, but a fourth component also has been described in healthy dogs<sup>2</sup>: wave A, retrograde; wave V, transient, which may be antegrade, retrograde, or neutral; and, 2 antegrade waves, named S and D.<sup>3</sup>

The A wave represents right atrial contraction; the S wave (the largest antegrade wave) occurs in ventricular systole, as the walls contract and the tricuspid annulus is directed to the apex, generating negative pressure and pushing blood out of the liver and the D wave occurs during passive filling of the atrium and right ventricle (RV) during diastole. Finally, the V wave is the result of atrial filling as systole becomes less intense and the tricuspid valve returns to its normal position.<sup>3</sup>

In veterinary medicine, spectral Doppler examinations of hepatic veins have been carried out. These investigations were used for the analysis of different hemodynamic conditions in healthy anesthetized dogs,<sup>4</sup> to estimate central venous pressure,<sup>5</sup> in patients with different degrees of tricuspid insufficiency,<sup>6</sup> as well in overweight and obese dogs.<sup>7</sup> However, this technique has not been widely used for assessment of the RV.

Spectral Doppler examination of hepatic veins may provide information regarding heart function. Our study was designed to assess the normal pattern of hepatic venous flow from Doppler ultrasound examination so as to characterize its spectral model. Additionally, we tried to correlate these data with structural and functional RV variables to determine if age, sex, body weight (BW) quartiles, heart rate (HR), cardiac rhythm, and systolic arterial pressure (SAP) affect the results in healthy dogs.

## 2 | MATERIALS AND METHODS

### 2.1 | Animals

This cross-sectional prospective observational study included 65 healthy client-owned dogs of different breeds and ages that were admitted to the Comparative Cardiology Laboratory of the Federal University of Paraná, Curitiba, Paraná, Brazil, between October 2017 and April 2018. All the dogs received a complete physical examination, measurement of SAP, abdominal ultrasound scan (to rule out structural liver disorders), as well as ECG and echocardiographic examinations. Trained observers indirectly measured SAP in all dogs using the Doppler technique, as described in the literature.<sup>8</sup> Several measurements were performed to obtain an average of 5 stable values. Electrocardiographic tracings were obtained over a period of 3 minutes.

Exclusion criteria were as follows: hypertensive and hypotensive animals (defined as SAP >160 and <80 mm Hg, respectively), and dogs with non-sinus arrhythmias and liver and heart diseases, either acquired and congenital. All procedures met the guidelines for Animals in Research: Reporting in vivo Experiments.

### 2.2 | Echocardiography

The echocardiographic examination was carried out in all animals without the use of sedatives, in the right and left lateral decubitus position, according to the recommendations of the Echocardiography Committee of the Specialty of Cardiology, American College of Veterinary Internal Medicine.<sup>9</sup> For the assessments described later, we used digital ultrasound equipment with multifrequency transducers of 4-12 MHz (Affiniti 50, Philips Medical Systems, Andover, Massachusetts).

Morphologic assessment of the RV involved the measurement, on 2-dimensional images of the 4-chamber apical area optimized for the RV, of the following parameters: (1) internal basal diameter, extending from the free wall to the interventricular septum, immediately below the tricuspid annulus; (2) average diameter, located at a midpoint between the ventricular apex and the tricuspid annulus, extending from the free wall to the interventricular septum; and, (3) length, covering the region from the ventricle peak to the tricuspid annular plane. All measurements were performed in diastole and systole (Figure 1A and B).

For systolic function of the RV, we determined the following parameters: (1) fractional area change (FAC%), which was calculated from the percentage difference between the systolic and diastolic areas of the RV, based on 2-dimensional images (Figure 1A and B); (2) tricuspid annular plane systolic excursion (TAPSE), represented by the longitudinal displacement of the tricuspid plane in images obtained in M-mode, with the cursor placed on the junction of the tricuspid plane and the RV free wall (Figure 1C); (3) longitudinal strain of the RV free wall basal, middle and apical segments, obtained by 2-dimensional speckle tracking (Figure 1D); and, (4) velocity of the tricuspid annulus systolic excursion (S'), quantified according to tissue Doppler imaging (TDI), with the cursor placed on the junction of the tricuspid plane and the RV free wall (Figure 1E). All parameters were quantified in 4 chamber apical views optimized for the RV. The images were obtained through the left parasternal window.

The structural variables of the RV (basal diameter, mean diameter, and length) and TAPSE also were indexed using body surface area (BSA; mm<sup>2</sup>) of the patients, which was obtained using the following formula:

$$BSA = K \times (BW \text{ in grams}^{2/3}) \times 10^{-4}.$$

$$K = \text{constant (10.1 for dogs)}.$$

Finally, for diastolic function of the RV, we determined the following parameters, based on the 4-chamber apical view optimized for this chamber: (i) profile of trans-tricuspid inflow velocity (waves E<sub>t</sub> and A<sub>t</sub>), using pulsed Doppler, with the cursor placed below the tricuspid valve (Figure 1F) and (ii) velocities of the tricuspid annulus systolic excursion in early and late diastole (E'<sub>t</sub> and A'<sub>t</sub>, respectively), which were quantified using TDI, with the cursor placed on the junction of the tricuspid plane and the RV free wall (Figure 1E).

**FIGURE 1** Measures for the morphofunctional assessment of the right ventricle (RV) obtained by means of echocardiography in 65 healthy dogs. A and B, Representation of structural measures of the RV, corresponding to the basal diameter (green line), average diameter (red line), and length (yellow line), in addition to the variation of fractional area of the RV (FAC%) (white line, dashed), in diastole and systole (respectively). C, Systolic excursion of the annular tricuspid plane (TAPSE). D, Two-dimensional longitudinal strain characterized by deformation graph of the basal, mid, and apical segments of the RV wall. E, Systolic excursion velocity of the tricuspid annular plane (S') and E' and A' waves representing the initial and late diastole, quantified by tissue Doppler imaging (TDI). F, Transtricuspid inflow, corresponding to E and A waves, which represent the initial and late diastole

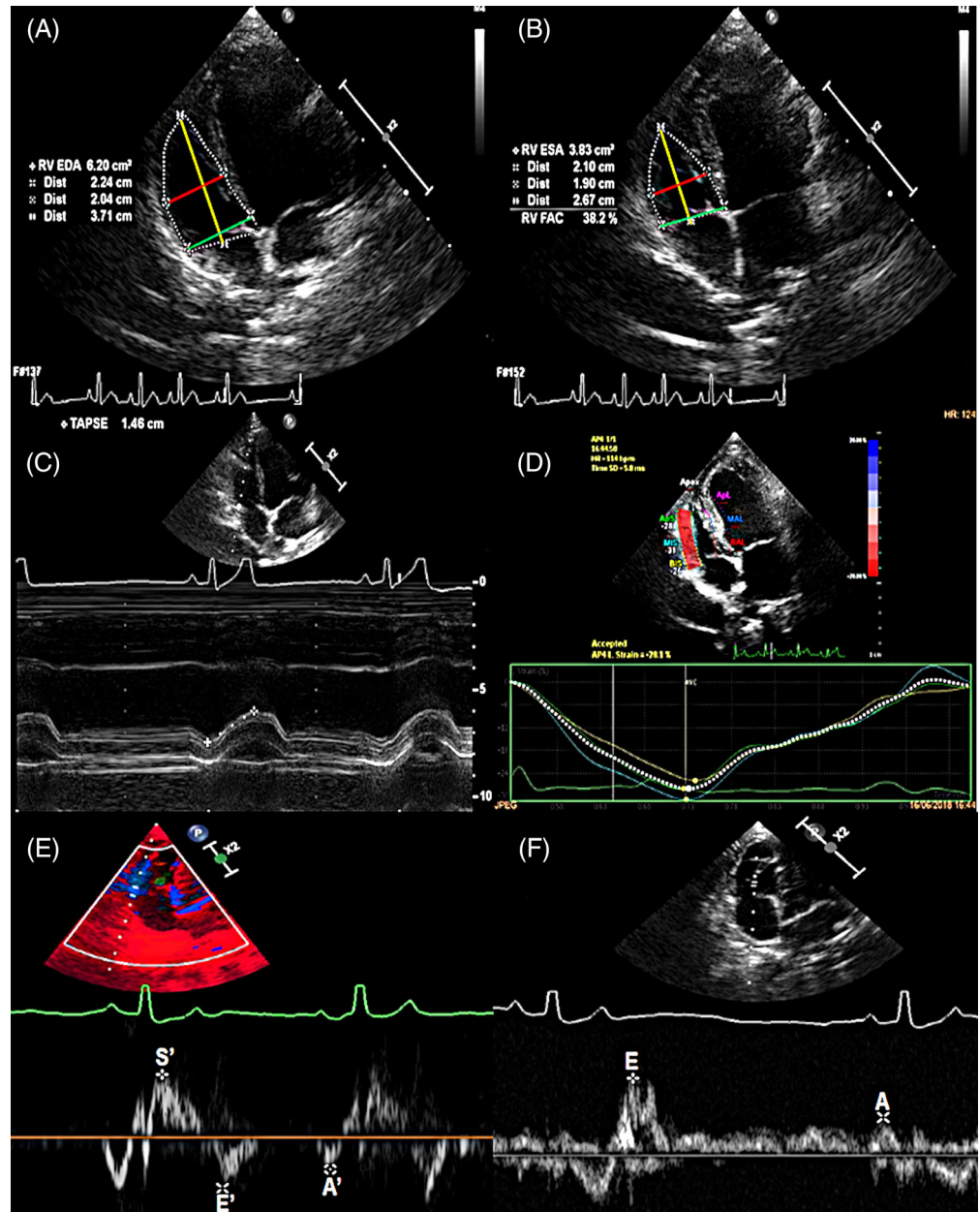


**TABLE 1** Comparison of different hepatic venous flow waves assessed by triplex Doppler according to body weight in 65 healthy dogs

n	Body weight (quartiles)				P-value
	2.0-8.15 kg	8.16-10.4 kg	10.41-17.0 kg	17.01-61.5 kg	
A Wave (cm/s)	7.0 (2.1) <sup>A</sup>	7.4 (2.3) <sup>A</sup>	9.0 (3.1) <sup>A</sup>	17.2 (10.1) <sup>B</sup>	<.001
S Wave (cm/s)	9.7 (1.9) <sup>A</sup>	11.9 (3.9) <sup>A</sup>	10.5 (2.0) <sup>A</sup>	18.5 (9.9) <sup>B</sup>	<.001
D Wave (cm/s)	7.3 (1.7) <sup>A</sup>	8.9 (3.7) <sup>A</sup>	7.7 (1.7) <sup>A</sup>	13.5 (8.5) <sup>B</sup>	.001
S/D*	1.3 (1.2-1.4) <sup>A</sup>	1.4 (1.2-1.5) <sup>A</sup>	1.3 (1.2-1.5) <sup>A</sup>	1.4 (1.2-1.7) <sup>A</sup>	.79

Note: Data are expressed as mean and SD, except for \* (nonparametric data), represented by median (quartiles). Values with different overlapping letters indicate a statistically significant difference between groups.

Abbreviations: n, number of animals per quartile; S/D, ratio S wave/D wave.

### 2.3 | Doppler spectrum of hepatic veins

To assess the triplex Doppler of hepatic veins, the dogs were placed in dorsal decubitus position and examined using digital ultrasound equipment with multifrequency transducers (both linear and convex) of 2-12 MHz (Affiniti 50, Philips Medical Systems). The ultrasonographic approach (subcostal) involved primarily the right medial and quadrate liver lobes, showing the right medial and quadrate hepatic veins. We used the gallbladder as a reference, because it provides a

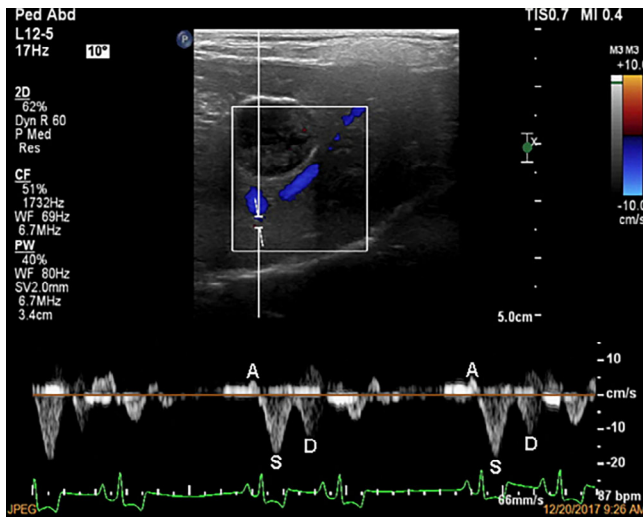


**FIGURE 2** Hepatic venous flow obtained by triplex Doppler of a healthy dog, characterized by the A, S, and D wave spectrum. S wave with higher velocity compared to D wave and consequent S wave/D wave ratio >1. Simultaneous electrocardiographic tracing facilitating the correct identification of the waves studied

parallel direction compared to Doppler, with angulations <60°. We differentiated portal veins from other veins based on the higher echogenicity of portal vein walls, and, for that reason, we did not assess them. A sample volume of 1 to 2 mm was used.

The direction and maximum velocity of 1 of the 4 possible components were determined from the pulsed-wave Doppler examination of the hepatic veins: (1) large negative anterograde wave during systole (S wave); (2) small positive retrograde wave during late systole (V wave); (3) anterograde wave during early diastole (D wave); or (4) retrograde wave during diastole after atrial contraction (A wave). Additionally, we established the ratio between the S wave and the D wave (S/D). We determined the beginning of each of the 4 phases based on cardiac electrical activity identified by the ECG tracing, which was obtained simultaneously with the B-mode ultrasound image and the use of pulsed-wave Doppler. The S wave occurs soon after the QRS complex, the V and D waves occur shortly after the T wave, and the A wave occurs immediately after the P wave of the ECG tracing. All examinations and measurements were performed by the same operator (V.B.C.S.).

### 2.4 | Intraobserver and interobserver variation and time requirements

To calculate intraobserver variation, 15 animals were reassessed by the same observer in the repeatability study, with a minimum interval of 30 days from the first assessment. The same studies were carried out by a coinvestigator (E.M.U.G.), blinded to the results of the first investigation, to measure interobserver variation. We also determined the time required for performing examinations in 8 dogs.

**TABLE 2** Comparison of the different indices of systolic and diastolic function of the right ventricle according to body weight in 65 healthy dogs

n	Body weight (quartiles)				P-value
	2.0-8.15 kg 16	8.16-10.4 kg 17	10.41-17.0 kg 16	17.01-61.5 kg 16	
Systolic indices					
FAC (%)	43.4 (10.3) <sup>A</sup>	43.4 (10.0) <sup>A</sup>	39.7 (7.3) <sup>A</sup>	37.3 (8.6) <sup>A</sup>	.16
TAPSE (mm)	9.7 (1.7) <sup>A</sup>	11.7 (2.8) <sup>AB</sup>	13.3 (2.9) <sup>B</sup>	16.8 (3.5) <sup>C</sup>	<.001
TAPSE (mm/m <sup>2</sup> )	35.7 (10.4) <sup>A</sup>	25.8 (6.4) <sup>B</sup>	24.8 (4.6) <sup>BC</sup>	18.6 (4.3) <sup>C</sup>	<.001
S* (cm/s)	11.2 (7.6-11.8) <sup>A</sup>	11.0 (10.1-14.0) <sup>AB</sup>	12.3 (11.2-15.9) <sup>AB</sup>	14.6 (12.1-16.9) <sup>B</sup>	.001
StL (%)	24.6 (3.8) <sup>A</sup>	22.7 (3.5) <sup>AB</sup>	22.1 (3.3) <sup>AB</sup>	20.4 (4.1) <sup>B</sup>	.02
Diastolic indices					
E <sub>t</sub> /A <sub>t</sub>	1.2 (0.4) <sup>A</sup>	1.4 (0.3) <sup>A</sup>	1.3 (0.3) <sup>A</sup>	1.5 (0.2) <sup>A</sup>	.09
E' <sub>t</sub> /A' <sub>t</sub> *	0.9 (0.6-1.2) <sup>A</sup>	1.3 (1.1-1.4) <sup>B</sup>	1.2 (1.0-1.2) <sup>AB</sup>	1.3 (1.1-1.4) <sup>B</sup>	.001

Note: Data are expressed as mean and SD (quartiles), except for \* (nonparametric data), represented by median (quartiles). Values with different overlapping letters indicate a statistically significant difference between groups.

Abbreviations: E<sub>t</sub>/A<sub>t</sub>, relation of the waves of the transtricuspid influx; E'<sub>t</sub>/A'<sub>t</sub>, relation of the systolic excursion of the tricuspid ring waves, in initial and late diastole, originating from the tissue Doppler; FAC, fractional area variation; n, number of animals per quartile; StL, longitudinal strain of the right ventricle; TAPSE, systolic excursion of the annular tricuspid plane.



## 2.5 | Statistical evaluation

The Shapiro-Wilk test was used to investigate the normality of data. Parametric and nonparametric data results, for both hepatic venous flow and morphology and function of the RV, are presented as mean, standard deviation (SD), and median (quartile), respectively. We divided the dogs into BW quartiles and compared them using analysis of variance followed by Tukey's test (for the parametric data), and the Kruskal-Wallis test followed by Dunn's test (for nonparametric data). The Kruskal-Wallis test was used to compare age with hepatic venous flow variables, whereas sex comparison was performed using the Mann-Whitney test. The Spearman test was used to investigate correlations between the data of the Doppler spectrum of the hepatic veins and age, SAP, HR, and RV structural and functional variables. Additionally, we calculated the coefficient of variation (CV) for the interobserver and intraobserver assessments and the mean duration of the examinations. All statistical analyses were performed using commercially available software (GraphPad Prism version 7.0.0, GraphPad Inc, La Jolla, California). We considered  $P < .05$  as significant.

## 3 | RESULTS

Sixty-five animals were recruited for the study, comprising a population of small-sized to large-sized dogs, including the following breeds: Beagle ( $n = 15$ ), German Shepherd ( $n = 5$ ), Pug ( $n = 3$ ), Border Collie, Lhasa Apso, Pekingese, Rottweiler, Whippet, Yorkshire Terrier (2 animals for each breed), French Bulldog, Chinese Crystal, Doberman Pinscher, Great Dane, Labrador, Belgian Malinois, Poodle, Shih-Tzu (1 animal for each breed), and crossbreed dogs ( $n = 20$ ). Of these, 24 were male (36.9%) and 41 were female (63.1%). Ages ranged between 4 and 156 months (mean, 45.2; median, 30), and BW from 2 to 61.5 kg (mean, 13.8; median, 10.4). The most common heart rhythm was sinus arrhythmia (83.1%), followed by sinus rhythm (10.7%) and sinus tachycardia (6.2%).

The values of the A, S, V, and D hepatic spectral waves varied according to the size of the animals. Significant statistical differences ( $P < .05$ ) were documented when BW quartiles were compared (Table 1). These results showed a positive relationship between BW quartiles and hepatic venous flow.

All animals had the same phase pattern for different waves: A and V retrograde waves (when present), and S and D anterograde waves, with higher velocities attributed to the S wave compared to the D wave (Figure 2). The mean of S/D ratio was  $\geq 1.2$  for the different BW quartiles, with no statistical differences when the interquartiles were compared (Table 1). The V wave was neutral in all but 3 dogs from the following experimental groups: 8.16-10.4 kg (3.5 cm/s), 10.41-17 kg (3.3 cm/s), and 17.01-61.5 kg (4.6 cm/s).

No correlation was observed between the waves of the hepatic venous flow and the S/D ratio with age and HR. However, the A wave showed a weak negative correlation with SAP ( $r_s: -0.25$ ;  $P = .04$ ), and a higher median value for hepatic spectral waves was found in males compared to females and a higher median value for hepatic spectral

waves was found in males compared to females, except for the S/D ratio.

Table 2 shows the comparisons between BW quartiles and the different indices of systolic and diastolic function of the RV. Significant differences ( $P < .05$ ) were observed between the BW quartiles (except for FAC% and  $E_t/A_t$ ), with increasing values with increases in BW for TAPSE (mm),  $S'$ , and  $E'_t/A'_t$ . In contrast, values for TAPSE (mm/m<sup>2</sup>) and longitudinal strain showed a negative correlation with BW. Several

**TABLE 3** Correlations between the hepatic venous flow assessed by triplex Doppler, and the indices of systolic function and diastolic right ventricle in 65 healthy dogs

	r	P-value
<b>A Wave (cm/s)</b>		
FAC (%)	-0.1842	.14
TAPSE (mm)	0.3921	.001
TAPSE (mm/m <sup>2</sup> )	-0.2028	.10
$S'$ (cm/s)	0.2939	.02
StL (%)	-0.1182	.34
$E_t/A_t$	0.3908	.001
$E'_t/A'_t$	0.3593	.001
<b>S Wave (cm/s)</b>		
FAC (%)	-0.1148	.36
TAPSE (mm)	0.2602	.03
TAPSE (mm/m <sup>2</sup> )	-0.1569	.21
$S'$ (cm/s)	0.3184	.001
StL (%)	-0.1298	.30
$E_t/A_t$	0.1720	.17
$E'_t/A'_t$	0.2810	.02
<b>D Wave (cm/s)</b>		
FAC (%)	-0.1055	.40
TAPSE (mm)	0.1671	.18
TAPSE (mm/m <sup>2</sup> )	-0.1514	.22
$S'$ (cm/s)	0.3144	.01
StL (%)	-0.0153	.90
$E_t/A_t$	0.1442	.25
$E'_t/A'_t$	0.2352	.06
<b>S/D</b>		
FAC (%)	0.0834	.50
TAPSE (mm)	0.0510	.68
TAPSE (mm/m <sup>2</sup> )	-0.0687	.58
$S'$ (cm/s)	-0.0976	.43
StL (%)	-0.0938	.45
$E_t/A_t$	0.0849	.50
$E'_t/A'_t$	0.0640	.61

Abbreviations: CI, confidence interval;  $E_t/A_t$ , transtricuspid influx waves ratio;  $E'_t/A'_t$ , ratio of systolic excursion of the tricuspid ring waves, in initial and late diastole, originating from tissue Doppler; FAC, fractional area variation; S/D, S wave/D wave ratio; StL, longitudinal strain of the right ventricle; TAPSE, systolic excursion of the annular tricuspid plane.

**TABLE 4** Comparison of different right ventricular structural indices in systole and diastole according to body weight in 65 healthy dogs

n	Body weight (quartiles)				P-value
	2.0–8.15 kg 16	8.16–10.4 kg 17	10.41–17.0 kg 16	17.01–61.5 kg 16	
Diastolic measurements					
Length (mm)	22.3 (4.6) <sup>A</sup>	32.6 (4.7) <sup>B</sup>	35.5 (6.4) <sup>B</sup>	48.6 (7.8) <sup>C</sup>	<.001
Length (mm/m <sup>2</sup> )	81.1 (19.7) <sup>A</sup>	71.7 (10.2) <sup>AB</sup>	66.3 (9.4) <sup>B</sup>	53.4 (7.) <sup>C</sup>	<.001
Basal diameter (mm)	14.7 (2.7) <sup>A</sup>	19.2 (4.0) <sup>B</sup>	22.6 (4.5) <sup>B</sup>	28.2 (3.9) <sup>C</sup>	<.001
Basal diameter (mm/m <sup>2</sup> )	53.9 (15.9) <sup>A</sup>	42.2 (8.2) <sup>B</sup>	42.4 (7.8) <sup>B</sup>	31.3 (5.8) <sup>C</sup>	<.001
Mean diameter (mm)	12.2 (2.3) <sup>A</sup>	16.0 (3.3) <sup>B</sup>	18.4 (3.8) <sup>B</sup>	23.4 (3.5) <sup>C</sup>	<.001
Mean diameter (mm/m <sup>2</sup> )	44.4 (10.8) <sup>A</sup>	35.3 (7.1) <sup>B</sup>	34.5 (6.8) <sup>B</sup>	26.2 (5.6) <sup>C</sup>	<.001
Systolic measurements					
Length (mm)	18.2 (6.3) <sup>A</sup>	23.9 (3.5) <sup>B</sup>	27.3 (4.8) <sup>B</sup>	38.1 (6.7) <sup>C</sup>	<.001
Length* (mm/m <sup>2</sup> )	63.1 (49.2–72.1) <sup>A</sup>	54.6 (48.7–59.1) <sup>A</sup>	51.9 (47.8–55.8) <sup>A</sup>	42.2 (37.0–44.9) <sup>B</sup>	<.001
Basal diameter (mm)	11.0 (2.1) <sup>A</sup>	16.4 (4.7) <sup>B</sup>	19.0 (4.4) <sup>B</sup>	23.1 (3.7) <sup>C</sup>	<.001
Basal diameter (mm/m <sup>2</sup> )	40.1 (11.6) <sup>A</sup>	36.0 (9.5) <sup>A</sup>	35.5 (7.7) <sup>A</sup>	25.8 (5.6) <sup>B</sup>	.001
Mean diameter (mm)	8.7 (1.7) <sup>A</sup>	12.7 (3.3) <sup>A</sup>	14.9 (3.5) <sup>A</sup>	18.9 (3.2) <sup>B</sup>	<.001
Mean diameter (mm/m <sup>2</sup> )	31.8 (8.8) <sup>A</sup>	27.8 (6.6) <sup>A</sup>	27.7 (5.6) <sup>A</sup>	21.3 (5.5) <sup>B</sup>	.001

Note: Data are expressed as mean and standard deviation (quartiles), except for \* (nonparametric data), represented by median (quartiles). Values with different overlapping letters indicate a statistically significant difference between groups.

Abbreviations: n, number of animals per quartile.

functional indices of the RV, such as TAPSE (mm),  $S'$ , and the ratios  $E_t/A_t$  and  $E'_t/A'_t$ , had weak positive correlation with the hepatic venous flow waves (Table 3). The  $S'$  wave weakly correlated with all hepatic spectral waves. On the other hand, the S/D ratio showed no correlation to these waves.

A significant difference ( $P < .05$ ) was found between all the structural parameters of the RV when compared to BW quartiles, with higher values as BW increased (Table 4). When BW was indexed to BSA, we found an inverted relationship. No correlation was found between morphometric data of the RV and hepatic venous flow.

Good repeatability was found for intraobserver and interobserver assessments of hepatic spectral flow. The CV values were moderately higher for the A, S, and D waves in the interobserver (CV, 10.7%, 17%, and 10.6%) compared to the intraobserver (CV, 2.7%, 10.5%, and 7.2%) analysis. The mean time for obtaining hepatic spectral wave measurements was 5.2 minutes. We had difficulty performing the examination in tachypneic and restless patients, but such characteristics did not prevent us from obtaining measurements.

## 4 | DISCUSSION

In people, assessment of hepatic venous flow and its association with right heart hemodynamics is well established.<sup>1</sup> This technique is uncommon in veterinary medicine. Our study has demonstrated the applicability of this technique and its feasibility with respect to detection, direction, velocity, and morphology of hepatic spectral waves and their relationship to BW. Furthermore, data related to morphology and function of the RV support the findings of the Doppler technique.

All the animals had a 3-phase pattern, characterized by the A, S, and D waves, with the exception of 3 dogs, in which the retrograde V wave was seen. These findings support those reported in a previous study.<sup>3</sup>

In normal hearts most anterograde blood flow occurs during ventricular systole, and consequently the S wave is larger than the subsequent D wave, with direct effects on the S/D ratio.<sup>10</sup> No significant difference was found in the comparison of the BW quartiles to the S/D ratio (Table 1). However, an increase in the values of A, S, and D waves was observed according to BW ( $P < .05$ ), possibly in response to the larger volumetric requirement involved. Values of the S/D ratio  $\geq 1.2$  were observed in the different BW ranges (Table 1), similar to previously findings.<sup>6</sup> Thus, it is possible to set an expected cutoff value for normality.

Body weight directly influenced the findings when compared to the functional variables of the RV (Table 2), as described in a previous study.<sup>11</sup> According to the authors, because several structural and functional echocardiographic indices (eg, body size) are affected, consideration must be given to provision of a more accurate assessment of reference intervals, given the wide range of dog sizes. In this context, TAPSE (in millimeters) is a linear measure and increases according to body dimensions.<sup>12</sup> However, when indexed to the BSA, an inversion of the results was observed (Table 2). One possible explanation is that, despite the larger values in millimeters, the percentage of annular displacement is lower in larger dogs, as observed in a study that assessed mitral annular movement.<sup>13</sup>

Comparison between functional RV indices and hepatic venous flow (Table 3) allowed for detection of a weak positive correlation

between  $S'$  and hepatic waves A ( $r_s$ : 0.29,  $P$ : .01), S ( $r_s$ : 0.31;  $P$ : .001), and D ( $r_s$ : 0.31,  $P$ : .01). The velocity of the tricuspid annulus systolic excursion is a fast, easy-to-execute, and strongly correlated variable for invasive hemodynamic measurement of the RV.<sup>14,15</sup> Therefore, values within the reference range for  $S'$ , in the absence of liver disease, make it a possible predictor for normal hepatic venous flow.

Values of RV morphometric indices increased with BW (Table 4). However, when the measurements were indexed to BSA, an inversion of results occurred. In humans, a survey involving a healthy multiethnic population showed that measurements of the RV in men exceeded absolute scores in females for 90% of measurements. However, once BSA was indexed, the values for women became significantly higher. Furthermore, indexation decreased the number of statistical differences among male ethnic groups.<sup>16</sup> Similarly, in dogs, although structural measurements of the RV of bigger dogs are larger, so is their BSA. Thus, proportionally, values when indexed to BSA become smaller when compared to small dogs.

The 3-phase hepatic wave pattern is produced during the final silent phase of inspiration. At this point, sufficient blood has returned to the heart through the hepatic veins to produce a normal waveform.<sup>17</sup> A study involving a healthy human population determined that hepatic vein velocities and waveforms varied during respiratory movements.<sup>18</sup> In our study, breathing had a direct influence on the Doppler study. In animals with tachypnea, artifactual waves were generated, and simultaneous ECG analysis was important in these cases. Excessive movement of the patient hinders the identification of hepatic veins.

In our study, repeatability was satisfactory between duplicate measurements, and intraobserver and interobserver variability was lower for the characterization of the hepatic spectral Doppler. This is important considering that it is a dynamic examination, susceptible to interference (such as unhealthy animals and panting), in addition to the relatively long time that elapsed (minimum interval of 30 days) from the first assessment.

In a single dog, examination took substantially longer (26 minutes). Both assessors found detection of hepatic waves in this animal difficult. In healthy dogs, the diameter of hepatic veins is small, and individual variation occurs. If this outlier is withdrawn from the analysis, the mean time for the examination would fall from 5.2 to 2.26 minutes.

Our study had some limitations. The animals were described as healthy based on clinical assessment and echocardiographic, ECG, and ultrasonographic examinations, as well as SAP measurements. However, asymptomatic comorbidities cannot be excluded, because specific complementary examinations were not performed. In addition, the number and variability of the animals may have been insufficient to extrapolate the results obtained to all breeds, and only the M mode (and not the bidimensional mode) was used to evaluate TAPSE.

Although the expected phasic pattern for hepatic venous flow in healthy dogs has already been described,<sup>2</sup> no studies have established reference ranges according to BW quartiles.

Because hepatopathies modify the hepatic venous flow pattern,<sup>1</sup> the results of our study provide a basis for future studies involving animals with changes that affect both the right side of the heart and

the liver. More studies regarding hepatic venous flow pattern could help the ultrasonographer distinguish between diseases that cause hepatic congestion because of local disturbance or in response to right-sided congestive heart failure. Thus, we propose that ultrasonography be considered as a complementary diagnostic modality, which allows objective referral for further complementary examinations.

## 5 | CONCLUSIONS

Hepatic spectral Doppler correlates with systolic and diastolic indices of the RV and varies according to BW. It is a technique with good repeatability and low variability, and future studies should validate the diagnostic applicability of this technique by assessment of its use in different diseases that affect the right heart.

## ACKNOWLEDGMENTS

We acknowledge the National Council of Scientific and Technological Development (CNPq) for the partial financial support represented by a postgraduate grant and the CAPA of the Federal University of Paraná for translation of the article.

## CONFLICT OF INTEREST DECLARATION

Authors declare no conflict of interest.

## OFF-LABEL ANTIMICROBIAL DECLARATION

Authors declare no off-label use of antimicrobials.

## INSTITUTIONAL ANIMAL CARE AND USE COMMITTEE (IACUC) OR OTHER APPROVAL DECLARATION

All procedures were approved by the Ethics Committee on Animal Use of the Federal University of Paraná (protocol 29-2017, approved on May 5th, 2017).

## HUMAN ETHICS APPROVAL DECLARATION

Authors declare human ethics approval was not needed for this study.

## ORCID

Vinicius Bentivoglio Costa Silva  <https://orcid.org/0000-0002-0232-272X>

## REFERENCES

1. Fadel BM, Alassas K, Husain A, Dahdouh Z, di Salvo G. Spectral Doppler of the hepatic veins in noncardiac diseases: what the echocardiographer should know. *Echocardiography*. 2015;32:1424-1427.

2. Szatmári V, Sótonyi P, Vörös K. Normal duplex Doppler waveforms of major abdominal blood vessels in dogs: a review. *Vet Radiol Ultrasound*. 2001;42:93-107.
3. McNaughton DA, Abu-Yousef MM. Doppler US of the liver made simple. *Radiographics*. 2011;31:161-188.
4. Smithenson BT, Mattoon JS, Bonagura JD, Abrahamsen EJ, Drost WT. Pulsed-wave Doppler ultrasonographic evaluation of hepatic veins during variable hemodynamic states in healthy anesthetized dog. *Am J Vet Res*. 2004;65:734-740.
5. Nelson NC, Drost WT, Lerche P, Bonagura JD. Noninvasive estimation of central venous pressure in anesthetized dogs by measurement of hepatic venous blood flow velocity and abdominal venous diameter. *Vet Radiol Ultrasound*. 2010;51:313-323.
6. Kim J, Kim S, Eom K. Pulsed-wave Doppler ultrasonographic evaluation of hepatic vein in dogs with tricuspid regurgitation. *J Vet Sci*. 2017;18:73-79.
7. Belotta AF, Teixeira CR, Padovani CR, et al. Sonographic evaluation of liver hemodynamic indices in overweight and obese dogs. *J Vet Intern Med*. 2018;32:181-187.
8. Acierno MJ, Brown S, Coleman AE, et al. ACVIM consensus statement: guidelines for the identification, evaluation, and management of systemic hypertension in dogs and cats. *J Vet Intern Med*. 2018;32:1803-1822.
9. Thomas WP, Gaber CE, Jacobs GJ, et al. Recommendations for standards in transthoracic two-dimensional echocardiography in the dog and cat. Echocardiography Committee of the Specialty of cardiology, American College of Veterinary Internal Medicine. *J Vet Intern Med*. 1993;7:247-252.
10. Abu-Yousef MM. Duplex Doppler sonography of the hepatic vein in tricuspid regurgitation. *AJR Am J Roentgenol*. 1991;156:79-83.
11. Visser LC, Scansen BA, Schober KE, Bonagura JD. Echocardiographic assessment of right ventricular systolic function in conscious healthy dogs: repeatability and reference intervals. *J Vet Cardiol*. 2015;17:83-96.
12. Núñez-Gil IJ, Rubio MD, Cartón AJ, et al. Determination of normalized values of the tricuspid annular plane systolic excursion (TAPSE) in 405 spanish children and adolescents. *Rev Esp Cardiol*. 2011;64:674-680.
13. Schober KE, Fuentes VL. Mitral annulus motion as determined by M-mode echocardiography in normal dogs and dogs with cardiac disease. *Vet Radiol Ultrasound*. 2001;42:52-61.
14. Hori Y, Kano T, Hoshi F, Higuchi S. Relationship between tissue Doppler-derived RV systolic function and invasive hemodynamic measurements. *Am J Physiol Heart Circ Physiol*. 2007;293:120-125.
15. Jurcut R, Giusca S, La Gerche A, et al. The echocardiographic assessment of the right ventricle: what to do in 2010? *Eur J Echocardiogr*. 2010;11:81-96.
16. Willis J, Augustine D, Shah R, Stevens C, Easaw J. Right ventricular normal measurements: time to index? *J Am Soc Echocardiogr*. 2012;25:1259-1267.
17. Scheinfeld MH, Bilali A, Koenigsberg M. Understanding the spectral Doppler waveform of the hepatic veins in health and disease. *Radiographics*. 2009;29:2081-2098.
18. Altinkaya N, Koc Z, Ulasan S, Demir S, Gurel K. Effects of respiratory manoeuvres on hepatic vein Doppler waveform and flow velocities in a healthy population. *Eur J Radiol*. 2011;79:60-63.

**How to cite this article:** Silva VBC, Rodrigues Froes T, Gil EMU, Wolf M, Lucina SB, Sousa MG. Characterization of Doppler spectrum of hepatic veins and correlation with structural and functional variables of the right ventricle in healthy dogs. *J Vet Intern Med*. 2020;34:45–52. <https://doi.org/10.1111/jvim.15665>